

In situ collector cleaning and extreme ultraviolet reflectivity restoration by hydrogen plasma for extreme ultraviolet sources

Daniel T. Elg, John R. Sporre, Gianluca A. Panici, Shailendra N. Srivastava, and David N. Ruzic

Citation: *Journal of Vacuum Science & Technology A* **34**, 021305 (2016); doi: 10.1116/1.4942456

View online: <http://dx.doi.org/10.1116/1.4942456>

View Table of Contents: <http://scitation.aip.org/content/avs/journal/jvsta/34/2?ver=pdfcov>

Published by the AVS: Science & Technology of Materials, Interfaces, and Processing

Articles you may be interested in

[Rare-earth plasma extreme ultraviolet sources at 6.5–6.7 nm](#)

Appl. Phys. Lett. **97**, 111503 (2010); 10.1063/1.3490704

[Lifetime measurements on collector optics from Xe and Sn extreme ultraviolet sources](#)

J. Appl. Phys. **102**, 023301 (2007); 10.1063/1.2756525

[Formation and direct writing of color centers in LiF using a laser-induced extreme ultraviolet plasma in combination with a Schwarzschild objective](#)

Rev. Sci. Instrum. **76**, 105102 (2005); 10.1063/1.2072147

[Radio-frequency discharge cleaning of silicon-capped Mo/Si multilayer extreme ultraviolet optics](#)

J. Vac. Sci. Technol. B **20**, 2393 (2002); 10.1116/1.1524153

[Characterization of Cu surface cleaning by hydrogen plasma](#)

J. Vac. Sci. Technol. B **19**, 1201 (2001); 10.1116/1.1387084



Instruments for Advanced Science

<p>Contact Hiden Analytical for further details: W www.HidenAnalytical.com E info@hiden.co.uk</p> <p>CLICK TO VIEW our product catalogue</p>	 <p>Gas Analysis</p> <ul style="list-style-type: none"> › dynamic measurement of reaction gas streams › catalysis and thermal analysis › molecular beam studies › dissolved species probes › fermentation, environmental and ecological studies 	 <p>Surface Science</p> <ul style="list-style-type: none"> › UHV TPD › SIMS › end point detection in ion beam etch › elemental imaging - surface mapping 	 <p>Plasma Diagnostics</p> <ul style="list-style-type: none"> › plasma source characterization › etch and deposition process reaction › kinetic studies › analysis of neutral and radical species 	 <p>Vacuum Analysis</p> <ul style="list-style-type: none"> › partial pressure measurement and control of process gases › reactive sputter process control › vacuum diagnostics › vacuum coating process monitoring
---	--	--	--	--

***In situ* collector cleaning and extreme ultraviolet reflectivity restoration by hydrogen plasma for extreme ultraviolet sources**

Daniel T. Elg

Department of Nuclear, Plasma, and Radiological Engineering, Center for Plasma-Material Interactions, University of Illinois at Urbana-Champaign, Urbana, Illinois 61801

John R. Sporre

Department of Nuclear, Plasma, and Radiological Engineering, Center for Plasma-Material Interactions, University of Illinois at Urbana-Champaign, Urbana, Illinois 61801 and IBM Corporation, Albany, New York 12203

Gianluca A. Panici

Department of Nuclear, Plasma, and Radiological Engineering, Center for Plasma-Material Interactions, University of Illinois at Urbana-Champaign, Urbana, Illinois 61801

Shailendra N. Srivastava

Applied Research Institute, University of Illinois at Urbana-Champaign, Champaign, Illinois 61820

David N. Ruzic^{a)}

Department of Nuclear, Plasma, and Radiological Engineering, Center for Plasma-Material Interactions, University of Illinois at Urbana-Champaign, Urbana, Illinois 61801

(Received 14 December 2015; accepted 4 February 2016; published 23 February 2016)

Laser-produced Sn plasmas used to generate extreme ultraviolet (EUV) light for lithography cause the release of Sn ions and neutrals in the EUV source chamber. These Sn atoms condense and deposit on the multilayer collector optic, which reduces its ability to reflect EUV light. This lowers the source throughput and eventually necessitates downtime for collector cleaning. In this paper, an *in situ* plasma-based collector cleaning technique is presented and experimentally demonstrated. First, the technique is shown to completely clean a 300 mm diameter stainless steel dummy collector. Second, simulations and secondary ion mass spectroscopy depth profiles show that the technique does not erode the real multilayer mirrors. Finally, EUV reflectivity measurements demonstrate the ability of the technique to restore EUV reflectivity to Sn-coated multilayer mirrors. This technique has the potential to be used in conjunction with source operation, eliminating cleaning-related source downtime. © 2016 American Vacuum Society.

[<http://dx.doi.org/10.1116/1.4942456>]

I. INTRODUCTION

In recent decades, massive advances have been made in the semiconductor industry by adherence to Moore's law, which states that the number of transistors on a single integrated circuit chip must double every two years.¹ In just 30 years, the minimum feature size on a chip has shrunk from 1 μm to 14 nm.² This progress has been enabled by consistent advances in optical lithography. Among the parameters which affect the minimum resolution of a lithography system is the wavelength of the light source used to pattern photoresist on Si wafers. Historically, that wavelength was near to or smaller than the minimum feature size.³ Since the adoption of the 193 nm excimer laser in 2001, however, the wavelength used in high-volume optical lithography has not decreased. Accordingly, there is a motivation to enable further size reduction by reducing the wavelength used in lithography.

In particular, research has focused on extreme ultraviolet (EUV) lithography, which uses a 13.5 nm light source. While EUV sources have shown remarkable progress in recent years,⁴ they cannot yet meet the required power and

availability for high-volume manufacturing (HVM). Additionally, after EUV has gained HVM insertion, source power requirements will continue to rise as the feature size continues to shrink.⁵

Both EUV power to the wafer and source availability are hampered by the need for collector cleaning. EUV photons are created by a dense ($T_e \sim 20 \text{ eV}$, $n_e \sim 10^{19} \text{ cm}^{-3}$) laser-produced Sn plasma.^{4,6,7} Due to the poor reflectivity and high transmissivity of all known solids, the optics which focus these photons must employ Bragg reflection by means of 7 nm-thick Mo/Si bilayers, which cause Bragg reflection of 13.5 nm light.⁸⁻¹⁰ Such optics are known as multilayer mirrors (MLMs). The first of these mirrors, the collector optic, is directly exposed to the EUV plasma, which deposits Sn on the collector and degrades EUV reflectivity (EUVR). While debris mitigation techniques such as magnetic mitigation (to deflect ions) and buffer gas (to deflect neutrals) exist,^{11,12} no debris mitigation technique can completely eliminate Sn deposition on the collector. Thus, as Sn accumulates, EUV power at the wafer is reduced until the collector must be either cleaned or replaced, incurring costs and downtime.

The best way to minimize downtime is to clean the collector while in the chamber (*in situ*). This can be accomplished

^{a)}Electronic mail: druzic@illinois.edu

with hydrogen radicals, which etch Sn by forming the gas SnH_4 . Hydrogen radicals have been previously shown to etch Sn.^{13,14} However, these experiments have been performed by utilizing a hot-filament radical source and then blowing the radicals at an Sn-coated sample. While this is a possible technique, its application to a real EUV system could necessitate the insertion of a delivery system in front of the collector (causing downtime) and could be subject to radical diffusion and recombination on the walls of the delivery system in the chamber.

The novel cleaning solution described in this paper is to create the radicals directly on the collector surface by using the collector itself to drive a capacitively coupled hydrogen plasma. This paper shows successful cleaning of a 300 mm stainless steel dummy collector optic by means of this technique, and the removal rates are measured. Simulations and secondary ion mass spectroscopy (SIMS) depth profiles are undertaken to show that the plasma does not erode different multilayer mirror surfaces. Finally, the technique is shown to restore EUV reflectivity to Sn-coated MLMs. The development of an *in situ* cleaning technique without a delivery system has the potential to run at the same time as the EUV source, enabling restoration EUV reflectivity and source power throughput without any cleaning-related downtime.

II. EXPERIMENTAL SETUP AND PLASMA SOURCE

Etching was performed in the Xtreme Commercial EUV Exposure Diagnostic (XCEED) chamber. XCEED, originally designed as a Xe-based discharge-produced EUV source, was repurposed to hold a stainless steel dummy collector optic. The collector was 300 mm in diameter and was isolated from the chamber ground with polytetrafluoroethylene clamps. The collector was attached, through a matching network, to a 300 W 13.56 MHz RF source, and a capacitively coupled hydrogen plasma was broken down on the surface of the collector. This plasma creates H radicals, as well as ions that can produce H radicals upon impact with the surfaces;¹⁵ the

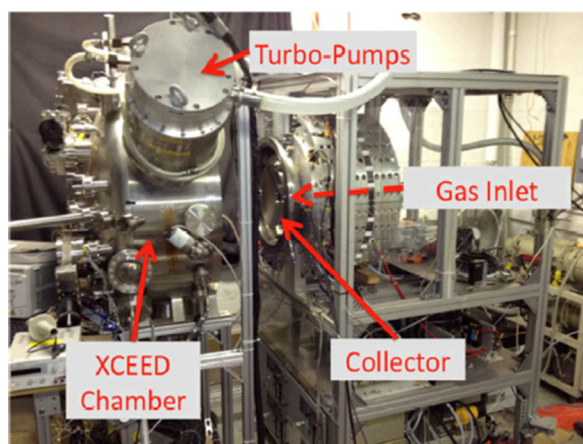


FIG. 1. (Color online) XCEED is shown with the collector installed. For etching experiments, the chamber (on the cart at left) was attached to the former EUV source (at right). The collector was driven with 300 W 13.56 MHz RF power through an electrical feedthrough, which allowed for electrical connection to the electrically isolated dummy collector.

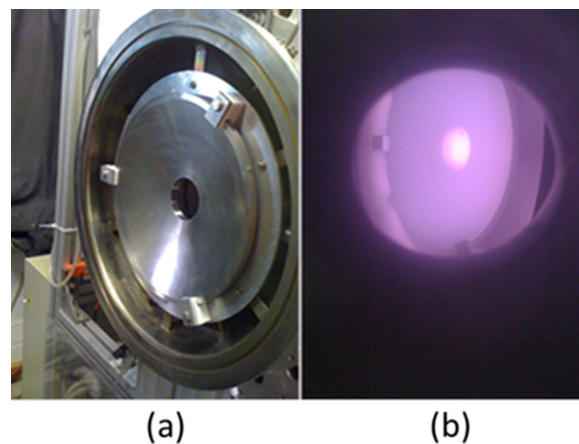


FIG. 2. (Color online) (a) Collector is installed with electrically isolating Teflon clamps. (b) The collector driving a hydrogen plasma, with the collector itself acting as the antenna.

radicals then reactively etch Sn by forming SnH_4 . For the experiments shown in this paper, the hydrogen pressure was 65 mTorr, and the flow rate was 500 sccm. The gas was injected through an inlet behind the center hole of the collector.

A picture of XCEED is shown in Fig. 1. Pictures of the dummy collector with and without a plasma are shown in Fig. 2. A circuit diagram is shown in Fig. 3.

Deposition was carried out in a separate chamber with a DC magnetron operating at 30 mA of current in approximately 3 mTorr of Ar. A quartz crystal monitor (QCM) was used to measure deposition thickness. The entire collector was coated with Sn. For removal rate experiments, masked Si witness plates were attached along a collector radius in order to yield measurements of local removal rate, as shown in Fig. 4. For experiments involving MLM samples, these samples instead were placed on the collector area and some bare Si area had been exposed to the plasma, while other parts of each area had not. This allowed for measurement of various interfaces by the profilometer. In particular, each sample was split into four quadrants, each of which had been exposed to a different set of conditions: “etched Sn” was coated with Sn and exposed to the etching plasma, “etched Si” was never coated with Sn but was exposed to the etching plasma,

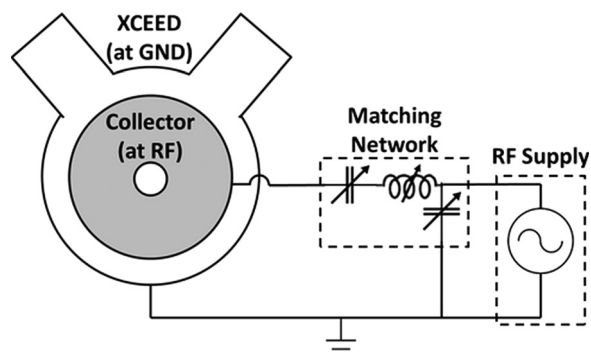


FIG. 3. Circuit diagram of the plasma source setup is shown. The collector is isolated inside XCEED and is attached to a 300 W 13.56 MHz RF supply. A matching network serves to minimize reflected power.

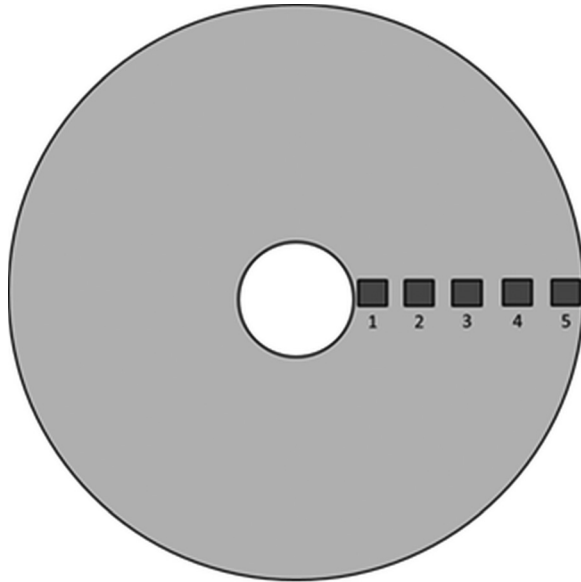


FIG. 4. Diagram of the collector is shown with Si witness plates attached in five different positions. The entire collector was coated with Sn during depositions; however, to measure local removal rates, Si witness plates were also placed on the collector during deposition and etching. These were later analyzed in a profilometer.

“masked Sn” was coated with Sn but not exposed to the etching plasma, and “masked Si” was never coated with Sn or exposed to the etching plasma. A diagram is shown in Fig. 5.

SEM and AFM were also used for characterization of certain samples. A Langmuir probe was used to determine plasma potential; theory and operation are described in Ref. 16. For MLM surface damage experiments, depth profiles were determined with SIMS to see if etching had removed the MLM capping layer. For EUV reflectivity experiments, the advanced light source synchrotron at Lawrence Berkeley National Laboratory was used to determine EUV reflectivity.

III. RESULTS AND DISCUSSION

A. Removal rate experiment

Sn removal experiments were carried out for initial depositions of 20, 50, 100, and 200 nm. Each etch was carried out for 2 h. After each experiment was completed, samples were taken to the profilometer and SEM for characterization.

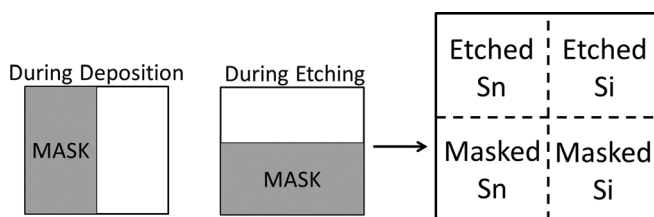
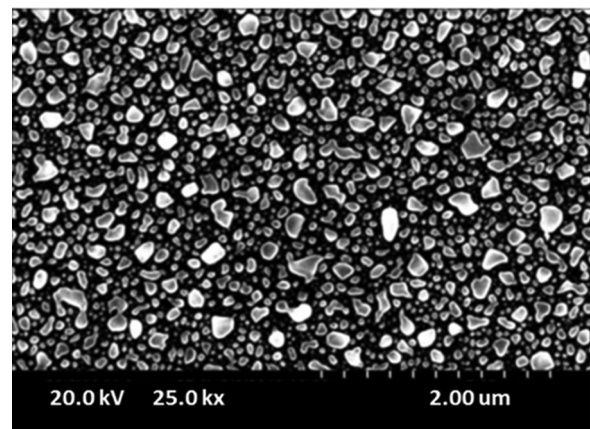


FIG. 5. Masking was employed during etching and deposition to yield four quadrants on each witness plate; each quadrant had been exposed to different conditions. “etched Sn” was coated with Sn and exposed to the etching plasma, “etched Si” was never coated with Sn but was exposed to the etching plasma, “masked Sn” was coated with Sn but not exposed to the etching plasma, and “masked Si” was never coated with Sn or exposed to the etching plasma.

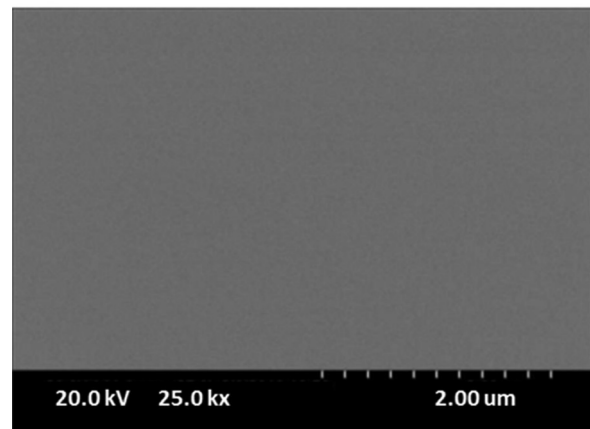
It is known that SnH_4 easily decomposes and redeposits Sn upon collision with metal surfaces.¹⁷ Despite Sn coverage of the entire collector, redeposition was not able to prohibit collector cleaning. Complete etches were observed for 20, 50, and 100 nm experiments. Profilometry indicated no difference in height between the etched Sn and etched Si quadrants. Additionally, SEM images indicated that the etched Sn quadrants were devoid of Sn and composed solely of pristine Si.

A comparison of the etched Sn quadrant and the masked Sn quadrant of a 20 nm sample is shown in Fig. 6. Figure 7 shows a backscattered electron image of all four quadrants of one of the 50 nm samples. This alternative SEM technique is sensitive not to topology but to material composition; thus, the fact that the Etched Sn quadrant appears to have the same darkness as the etched Si quadrant is indicative of a complete etch.

When coated with 200 nm of Sn, the collector was not completely cleaned after 2 h of etching. Due to incomplete etching, removal rates could be calculated. Witness plates analyzed on the profilometer yielded the removal rates shown in Fig. 8. Two scans were taken for each sample.



(a)



(b)

FIG. 6. SEM images show the difference between the plasma-cleaned section of a witness plate and the section that was coated with Sn but not exposed to plasma. (a) The masked Sn quadrant shows grains of deposited Sn, indicating the condition of the surface before etching. (b) The etched Sn quadrant, which was formerly Sn-coated, appears pristine after plasma cleaning.

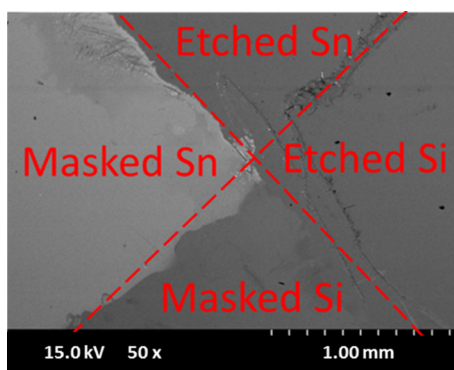


Fig. 7. (Color online) Backscattered SEM image, which is sensitive to material composition rather than topography, shows the etched Sn quadrant to be identical to the Si quadrants after 2 h of etching a 50 nm deposition. This provides further indication of a complete etch.

The removal rate nonuniformity may be explained by means of the redeposition phenomenon. Gas flows in through the center hole of the collector, which is closest to position 1; therefore, higher local flow velocities near sample 1 help to remove SnH_4 from the vicinity of that sample, decreasing redeposition. Additionally, sample 1 is not surrounded by Sn on all sides; thus, the localized source of redepositing Sn in the vicinity of sample 1 is lessened. Flow generally decreases as the distance from the center hole increases; however, it rises again at position 5. This is due to the fact that position 5 is also near an edge of the collector, lessening the local source of redepositing Sn.

B. MLM surface damage simulations and experiment

Since full-collector cleaning had been demonstrated and measured, it was relevant to know if exposure to the plasma would pose a threat to an actual MLM surface. As an initial indicator, an AFM scan on the etched Si quadrant of one of

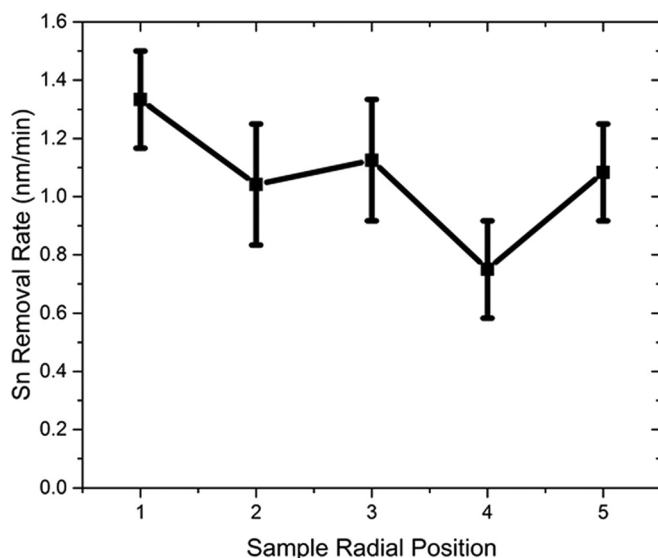


Fig. 8. Removal rates are shown at 65 mTorr, 500 sccm for each sample according to the sample positions diagrammed in Fig. 4. Rates are higher near the edges of the collector due to flow near position 1 and the fact that position 1 and position 5, being on the edges, are not surrounded by Sn on all sides.

the 200 nm samples revealed that, after spending 2 h exposed to the etching plasma, the etched Si quadrant had a roughness of only 3.2 Å. Such a low roughness is close to the typical roughness value for a polished and very-carefully handled Si wafer, 1.5 Å.¹⁸ Such a small increase in roughness can be attributed to the fact that the sample was handled and cut outside a cleanroom; thus, the measured value of 3.2 Å does not indicate plasma-caused surface damage.

A deeper investigation of surface damage was undertaken through stopping and range of ions in matter (SRIM) modeling and SIMS depth profiles of plasma-cleaned MLM samples. First, to give an estimate of possible ion energies, the voltage curve on the collector was measured to have an amplitude of approximately 700 V and a self-bias DC offset of about -300 V (such a self-bias is typical of the smaller electrode in capacitive RF plasma sources¹⁹). Plasma potential measured with a Langmuir probe was approximately 50 V. Thus, the ion energy was predicted to be on the order of 350 V on average.

Sputtering simulations were performed using SRIM.²⁰ Simulations were carried out for 99 999 flights of 350 eV H^+ ions on Si, Mo, Ru, and Zr. The first two elements comprise the actual MLM structure, and the latter two are often used in capping layers. The results, shown in Table I, indicate an incredibly small expected sputtering rate for Si and an expected rate of 0 for sputtering of Mo, Ru, and Zr.

It should be noted that, in discharges at this pressure, H_3^+ is often the dominant ion, while H_2^+ is present only in small numbers.²¹ Energetically, these multiatomic molecules may be thought of as individual H atoms with the total energy divided equally among them. Thus, sputtering yields of H_2^+ and H_3^+ are determined by those from H^+ ions with 1/2 or 1/3 of the energy, respectively. Simulations of H^+ sputtering at those energies produced no sputtering yield.

To experimentally verify the ability of MLM surfaces to withstand exposure to the hydrogen plasma, MLM samples were obtained. While all samples contained the same multi-layer structure, some had a capping layer of ZrN, while others had a capping layer of SiN. In order to test the effect of plasma on the samples, the samples were split into four groups: bare (never exposed to plasma), etched (exposed to the etching plasma), deposited (coated with Sn), and deposited and etched (coated with Sn and then etched). All etches were carried out for 45 min.

For all samples, a depth profile was obtained for each group by means of SIMS. In SIMS, the sample surface was

TABLE I. SRIM code is used to run sputtering simulations for common materials in EUV MLMs. The incident ion energy is set to 350 eV, the average incident energy of ions in the *in situ* plasma source. Simulations show a very low sputtering yield for Si and no sputtering yield for Mo, Ru, and Zr. Thus, the simulations indicate that little or no surface removal should be caused by the plasma cleaning technique.

	Si	Mo	Ru	Zr
Sputtering yield	0.021 at/ion	0	0	0
Sputtering rate	0.036 nm/min	0	0	0
Thickness sputtered after 45 min	1.6 nm	0	0	0

bombarded at normal incidence with 12 keV oxygen ions, sputtering off both neutral atoms and ions; these sputtered ions were then analyzed in a quadrupole mass spectrometer while recording the time. At such a high energy, the normal incidence sputtering rate can be assumed to be approximately constant for each material. After SIMS profiling, the crater created by ion bombardment was measured with a profilometer. Assuming material-independent sputtering rate, the total crater depth can be used to convert sputtering time into an approximate depth. Given this approximation, the depth numbers are more useful as a metric of comparison between multiple SIMS experiments, rather than measurements of absolute depth. It is also important to note that ionization yield, as opposed to sputtering yield, is very material-dependent. The secondary ion count measured by SIMS cannot be used to provide an absolute measure of elemental concentration in the sample; however, it may be used to show differences in relative concentration of a given element at different depths.

SIMS depth profiles of all ZrN-capped samples are shown in Fig. 9. All show a ZrN capping layer followed by multilayers of Mo/Si. While the plots are zoomed-in to highlight the profile near the surface, all profiles were carried out until a drop in Mo was observed, indicating the transition to the Si substrate beneath the multilayer structure. Oscillations in the Mo/Si counts are observed and indicate the presence of multilayers, though some smoothing is shown due to intermixing caused by heating from ion bombardment.

All samples in Fig. 9 show the same Zr capping structure of the same thickness, indicating that exposure to the hydrogen plasma has not damaged the surface of the MLM. All

ionization counts have been normalized to the value of the Si signal at 40 nm. Zr levels observed after the rise of Si fall below the noise floor of the instrument. The presence of a gradual Zr fall-off, rather than a sharp decrease, is due to intermixing caused by heating from the 12 keV ion beam; this also smoothens the Si and Mo profiles, rather than allowing them to be seen as discrete isolated peaks every 3.5 nm.

The absence of measurable removal is in agreement with the SRIM predictions. A small coating of Sn is seen on the deposited sample, while it is removed on the deposited and etched sample. However, the removal of Sn is the only difference between the two, indicating no observable damage to the MLM. It should be noted that, beyond the first few nanometers of the deposited sample, the Sn signal is at noise levels.

SIMS depth profiles were also carried out for SiN-capped samples. Similar results were observed; the capping layer was observed as a consistent bump in the Si count. Similarly, no surface erosion was observed.

C. EUV reflectivity restoration

While SIMS experiments established reasonable confidence in the lack of removal of non-Sn materials, the ultimate mark of a successful MLM cleaning technique is the ability to restore EUVR. The ZrN-capped and SiN-capped MLM samples were prepared and exposed to conditions similar to those in Sec. III B. Multiple sets of SiN-capped samples were used, but difficulty in obtaining ZrN-capped samples resulted in experiments being carried out for only one set of ZrN-capped samples. The only difference from the conditions in Sec. III B was the differentiation between

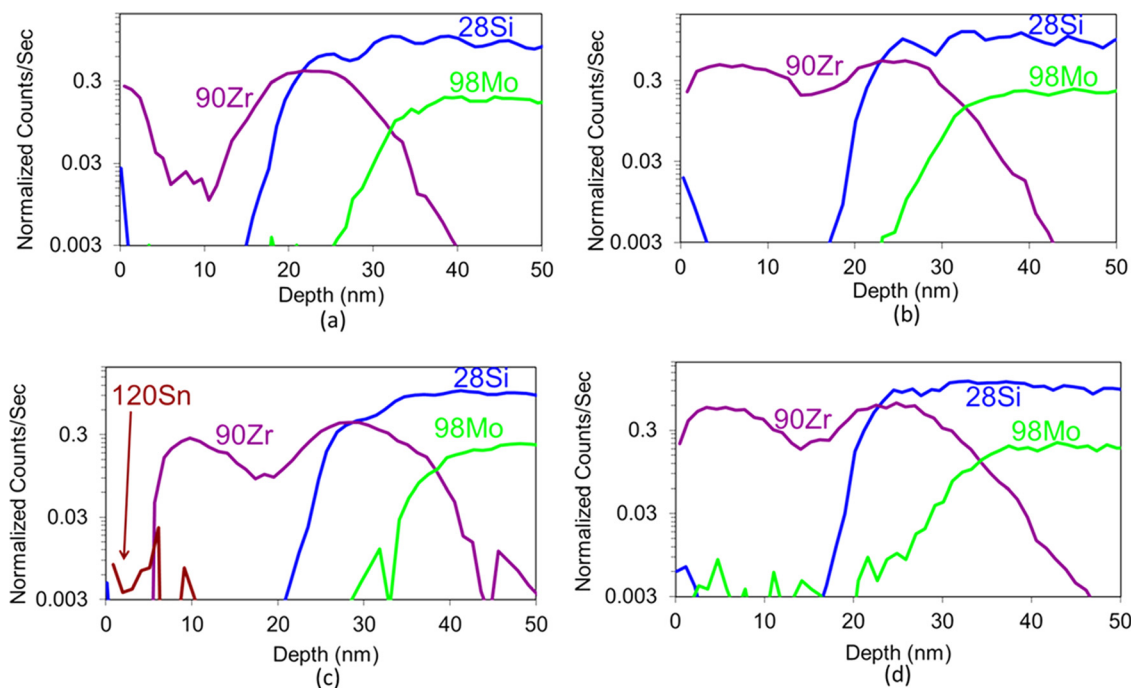


Fig. 9. (Color online) SIMS depth profiles are shown of (a) bare: A bare ZrN-capped MLM sample, (b) etched: A ZrN-capped sample exposed to the etching plasma for 45 min, (c) deposited: A Sn-coated ZrN-capped MLM sample, and (d) deposited and etched: A ZrN-capped sample that was coated with Sn but then exposed to the etching plasma for 45 min. All samples show the same capping layer structure and thickness, followed by the same multilayer structure. Thus, no damage or surface erosion is observed after 45 min. The only difference is the presence of a Sn layer in (c), which is removed by etching in (d).

“control” and “bare” samples. The control samples were never removed from their initial sample holders, while the bare samples were removed and handled but never placed in any plasma chamber. The purpose of this distinction was to quantify and isolate any potential reductions in reflectivity caused by atmospheric contaminants and handling.

Results from the ZrN-capped set are shown in Fig. 10. Error bars of $\pm 1\%$ have been added, based on the variability seen in multiple SiN-capped control samples (which will be shown later in Fig. 11).

As seen in Fig. 10, exposure and handling seem to have a minimal effect on the samples’ reflectivity, since the control and bare samples are within error bars of each other (50% vs 49%). No reflectivity loss is caused by the 45 min plasma exposure, as seen by the etched sample, which actually has a reflectivity that is well within an error bar and even nominally higher than the bare sample. Deposition predictably lowers reflectivity to a nonuseful value (approximately 6%). Finally, etching of a deposited sample brings the reflectivity back to 46%. While this value is slightly below the etched and bare values, such a result was expected due to contamination in the deposition experiment, which introduced small amounts of nonreflecting material to the surface. Thus, the results in Fig. 10 demonstrate the ability to restore EUV reflectivity to ZrN-capped MLM samples without causing damage to MLM surfaces exposed to the plasma.

As a comparison, the SiN-capped samples show a different pattern that indicates a detrimental effect caused by the plasma. As shown in Fig. 11, the etched samples lose approximately 10% reflectivity (from approximately 55% to approximately 45%) after simple exposure to the etching plasma. The

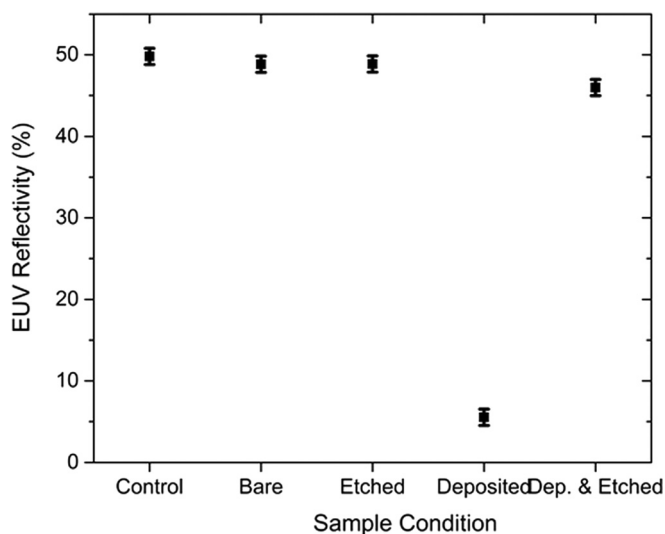


Fig. 10. ZrN-capped samples were exposed to five different conditions. The atmosphere did not appear to contaminate the samples, as is evident from the negligible difference in reflectivity between the control and bare samples. Exposure of a nondeposited sample to the etching plasma for 45 min yielded little surface damage, as evidenced by the reflectivity measurement of the etched sample. As expected, a deposition of 20 nm of Sn reduces the reflectivity drastically (deposited sample). Finally, the deposited and etched (“dep and etched”) sample was once coated with Sn but saw most of its reflectivity restored by *in situ* hydrogen plasma cleaning. Larger error bars on the last two samples are due to the presence of contamination in the deposition experiment.

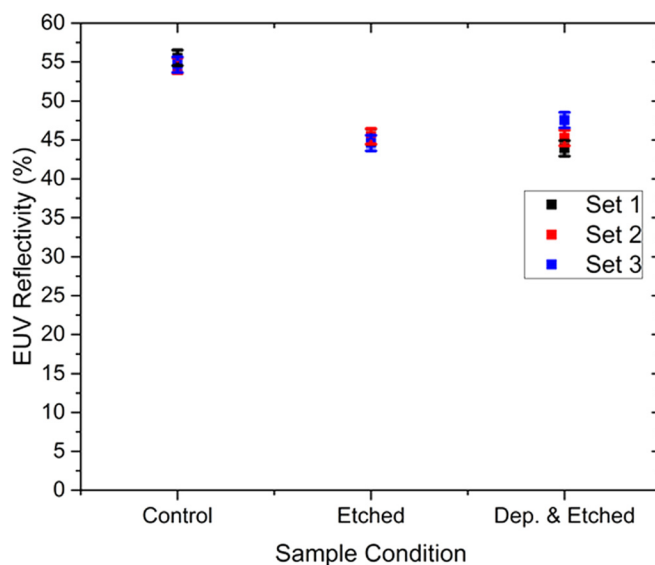


Fig. 11. (Color online) SiN-capped samples were exposed to the same conditions as the ZrN-capped samples. Due to an excess of supply, three sets of SiN-capped samples were exposed and measured. Due to time constraints at the synchrotron, only three different conditions were measured for EUVR. Etching does restore much reflectivity, since a sample with an Sn coating ought to have a reflectivity in the single digits, as was the case for the ZrN-capped deposited sample. However, it seems that any sample exposed to the etching plasma sees a final reflectivity of about 46%, which is 10% below the initial value of 56%. This effect is due to blistering on SiN-capped samples.

deposited and etched samples have approximately the same reflectivity, indicating reflectivity restoration ability (the values for the deposited samples and bare samples were not measured due to time constraints at the synchrotron). However, it seems that any samples exposed to the etching plasma see a reflectivity degradation from 55% to 45%. Due to the greater availability of the SiN-capped samples, experiments were performed on three sets of samples. To quantify the error in the EUVR measurements, a comparison was made between the measured reflectivities of the SiN-capped control samples. As seen in Fig. 11, the reflectivity variation was approximately 1%; therefore, the error bars for the EUVR measurements have been set to 1% EUVR.

As expected, SEM analysis confirmed that Sn removal was completed. However, SEM images of SiN-capped samples, shown in Fig. 12, display blisters, which are not seen on ZrN-capped samples after plasma exposure (Fig. 13).

It is concluded that the drop in reflectivity on SiN-capped MLMs (not seen on ZrN-capped MLMs) is due to hydrogen blistering. Hydrogen ions incident on the surface can implant, reacting with the Si or recombining to form H_2 . However, the native oxide on an SiN surface is known to present a hydrogen diffusion barrier.²² This keeps the implanted hydrogen from diffusing out; instead, it forms H_2 bubbles that cause blisters, which eventually rupture. ZrN does not show this same behavior; even after 45 min of direct exposure to the etching plasma, the sample in Fig. 13 did not show any signs of blistering.

It should be noted that current EUV source technology uses H_2 as a buffer gas to slow down high-energy Sn ions.¹²

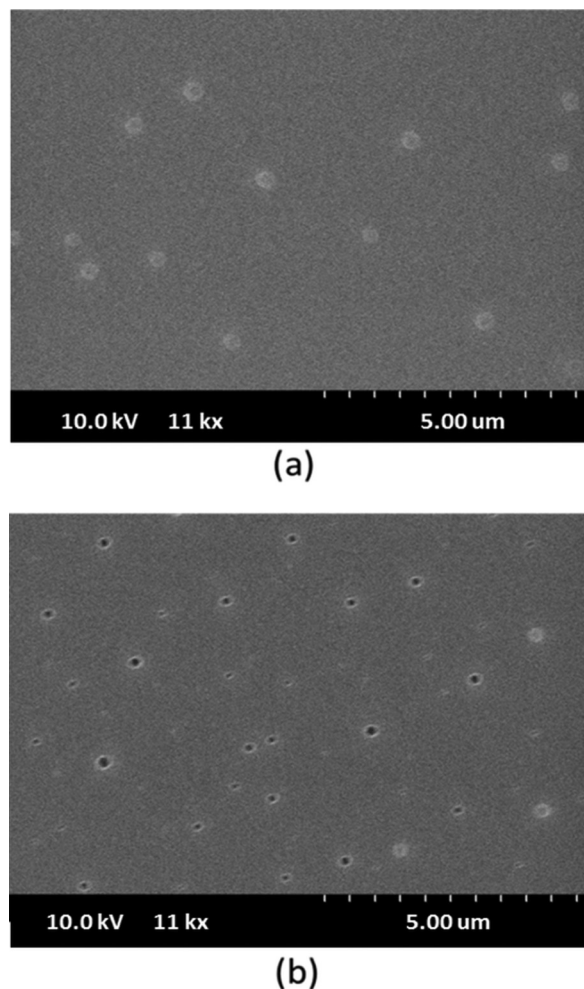


FIG. 12. Blistering is shown on SiN-capped samples after plasma exposure. (a) A deposited and etched sample shows blisters. (b) The surface of the etched sample was exposed to the etching plasma for longer than that of the deposited and etched sample, since the etched sample never had any Sn coating. On this sample, some of the blisters have burst.

Due to the radiation from the EUV plasma, some of this H_2 gas is dissociated and ionized, even if the collector is not driving a plasma. ZrN is known to be more stable than SiN in this environment.²³ Thus, since any commercial EUV collector will have to contend with a hydrogen plasma, ZrN is a likelier capping layer for commercial-level collectors. Accordingly, the ability of the technique shown in this paper to restore EUV reflectivity to ZrN-capped MLMs without damaging the capping layer or MLM structure indicates this technique's potential for adoption in commercial EUV sources.

IV. CONCLUSIONS

An *in situ* hydrogen plasma cleaning source for Sn removal in EUV sources has been proposed and demonstrated. This source uses the EUV collector optic to drive a capacitively coupled H_2 plasma, which produces H radicals that etch Sn as SnH_4 . A 300-mm-diameter stainless steel dummy collector has been coated with Sn and completely cleaned. Removal rates of approximately 1 nm/min have been measured. SRIM simulations and SIMS depth profiles have shown

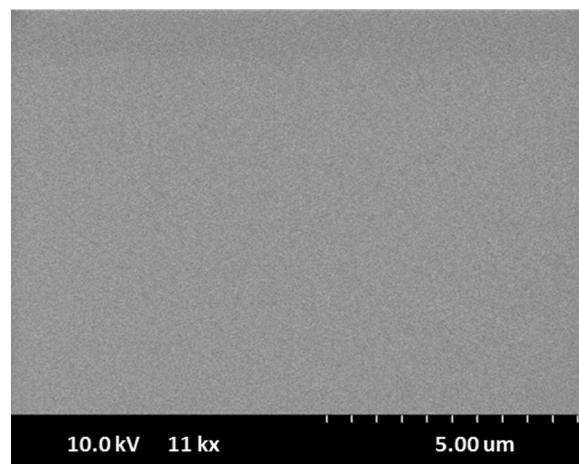


FIG. 13. Blistering is not seen on the ZrN-capped samples. The ZrN-capped etched sample, shown at the same magnification as the SiN-capped samples in Fig. 12, does not have any blisters.

that the technique does not cause sputtering of multilayer mirror surfaces. EUV reflectivity measurements have shown the ability of this technique to restore EUV reflectivity to Sn-coated multilayer mirror samples. Additionally, this technique appears to be compatible with ZrN-based capping layers.

Such a technique offers potential for scaling to a commercial EUV source and could use H_2 buffer gas already present in the chamber. If implemented industrially, this technique could yield on-demand *in situ* Sn cleaning for collector life extension without requiring a radical delivery system or EUV source downtime. This scaling will require further understanding of the radical creation mechanisms, the etching probability, the SnH_4 decomposition probability, and how to balance pressure and flow to achieve optimal Sn removal. These studies will be the subject of future publications.

ACKNOWLEDGMENTS

This material is based upon work supported by the National Science Foundation under Grant No.14-36081. Additionally, the authors are grateful for funding and support from Cymer, LLC. The authors would also like to thank Eric Gullikson of Lawrence Berkeley National Laboratory for performing the EUVR measurements. Parts of this research were carried out in the Frederick Seitz Materials Research Laboratory Central Facilities, University of Illinois, which is partially supported by the U.S. Department of Energy under Grant Nos. DEFG02-07ER46453 and DE-FG02-07ER46471.

¹G. E. Moore, *Int. Electron Devices Meet.* **21**, 11 (1975).

²S. Novak *et al.*, *Int. Reliab. Phys. Symp.* **53**, 2.F.2 (2015).

³M. Rothschild *et al.*, *Lincoln Lab. J.* **14**, 221 (2003).

⁴A. A. Schafgans *et al.*, *Proc. SPIE* **9422**, 94220B (2015).

⁵E. R. Hosler, O. R. Wood, W. A. Barletta, P. J. S. Mangat, and M. E. Preil, *Proc. SPIE* **9422**, 94220D (2015).

⁶J. Sporre and D. N. Ruzic, *J. Micro/Nanolith. MEMS MOEMS* **11**, 021117 (2012).

- ⁷R. A. Burdt, Y. Tao, M. S. Tillack, S. Yuspeh, N. M. Shaikh, E. Flaxer, and F. Najmabadi, *J. Appl. Phys.* **107**, 043303 (2010).
- ⁸D. T. Attwood, *Soft X-rays and Extreme Ultraviolet Radiation* (Cambridge University, Cambridge, England, 1999).
- ⁹H. Maury *et al.*, *Thin Solid Films* **514**, 278 (2006).
- ¹⁰C. Hecquet *et al.*, *Proc. SPIE* **6586**, 65860X (2007).
- ¹¹D. T. Elg, J. R. Sporre, D. Curreli, I. A. Shchelkanov, D. N. Ruzic, and K. R. Umstadter, *J. Micro/Nanolithogr. MEM* **14**, 013506 (2015).
- ¹²I. V. Fomenkov *et al.*, *Proc. SPIE* **7636**, 763639 (2010).
- ¹³M. M. J. W. van Herpen, D. J. W. Klunder, W. A. Soer, R. Morris, and V. Banine, *Chem. Phys. Lett.* **484**, 197 (2010).
- ¹⁴D. Ugur, A. J. Storm, R. Verberk, J. C. Brouwer, and W. G. Sloof, *Chem. Phys. Lett.* **552**, 122 (2012).
- ¹⁵M. Sode, T. Schwarz-Selinger, and W. Jacob *J. Appl. Phys.* **114**, 063302 (2013).
- ¹⁶D. N. Ruzic, *Electric Probes for Low-Temperature Plasmas* (AVS, New York, 1994).
- ¹⁷D. Ugur, A. J. Storm, R. Verberk, J. C. Brouwer, and W. G. Sloof, *Appl. Surf. Sci.* **288**, 673 (2014).
- ¹⁸L. W. Shive and B. L. Gilmore, *Electron Soc. Trans.* **16**, 401 (2008).
- ¹⁹M. A. Lieberman and A. J. Lichtenberg, *Principles of Plasma Discharges and Materials Processing*, 2nd ed. (Wiley, Hoboken, NJ, 2005).
- ²⁰J. F. Ziegler, J. P. Biersack, and M. D. Ziegler, *SRIM – The Stopping and Range of Ions in Matter* (Lulu, Morrisville, NC, 2008).
- ²¹I. Mendez, F. J. Gordillo-Vazquez, V. J. Herrero, and I. Tanarro, *J. Phys. Chem. A* **110**, 6060 (2006).
- ²²J. Catoir, W. Wolke, P. Hartmann, E. Gernot, R. Preu, R. Trassl, and S. Wieder, *23rd European Photovoltaic Solar Energy Conference* (2008), pp. 1542–1545.
- ²³A. I. Ershov, N. R. Bowering, B. La Fontaine, and S. De Dea, U.S. patent WO2014055308A1 (10 April 2014).